

COMPARISON BETWEEN INTERMODULATION DISTORTION PREDICTION CAPABILITIES OF THE COBRA MODEL AND OF OTHER NON-LINEAR FET MODELS

Vicentiu I. Cojocaru, Thomas J. Brazil

Microwave Research Group
Department of Electronic and Electrical Engineering
University College Dublin, Dublin 4, Ireland.
E-mail: vivi@hertz.ucd.ie

ABSTRACT

The paper presents results from a study carried out on two FET processes, to demonstrate the enhanced prediction capabilities of the general-purpose FET model COBRA [1], to predict the intermodulation distortion (IMD) characteristics of μ -wave and mm-wave FETs, in comparison with other traditional large-signal models. The first, second and third order derivatives of the COBRA I/V model function are analysed and compared with the corresponding functions for the Statz-Raytheon and a modified Materka model. For the COBRA model case, these derivatives are shown to be continuous over the entire bias plane and in agreement with experimental results previously presented in literature for similar devices and extracted from harmonic measurements. In the case of the other two models, the high-order derivatives are described less accurately, especially around critical bias regions such as knee, pinch-off or soft breakdown. A sequence of two-tone (IMD) large-signal test results are presented for the case of a 0.2 μ m PHEMT process designed for mm-wave applications, and operating in four different bias conditions. The results prove the advantages of the COBRA model in comparison with the other two in predicting high order IM products.

INTRODUCTION

It has been demonstrated in recent years [2][3][4] that there is a direct connection between the capability of a FET model to correctly predict IMD characteristics and the model's ability to reproduce the behaviour of the derivatives of the main I/V and Q/V characteristics. These non-linear characteristics are expressed via Taylor series expansions as follows:

$$\begin{aligned} I_{ds}(V_{gs}, V_{ds}) &= I_{ds}(V_{GS}, V_{DS}) + \frac{\partial I_{ds}}{\partial V_{gs}} v_{gs} + \frac{\partial I_{ds}}{\partial V_{ds}} v_{ds} + \frac{\partial^2 I_{ds}}{\partial V_{gs}^2} v_{gs}^2 + \frac{\partial^2 I_{ds}}{\partial V_{gs} \partial V_{ds}} v_{gs} \cdot v_{ds} + \frac{\partial^2 I_{ds}}{\partial V_{ds}^2} v_{ds}^2 + \dots = \\ &= I_{ds}(V_{GS}, V_{DS}) + Gm \cdot v_{gs} + Gds \cdot v_{ds} + Gm2 \cdot v_{gs}^2 + Gmd \cdot v_{gs} \cdot v_{ds} + Gd2 \cdot v_{ds}^2 + \\ &\quad + Gm3 \cdot v_{gs}^3 + Gm2d \cdot v_{gs}^2 \cdot v_{ds} + Gmd2 \cdot v_{gs} \cdot v_{ds}^2 + Gd3 \cdot v_{ds}^3 + \dots \end{aligned} \quad (1)$$

where $I_{ds}(V_{GS}, V_{DS})$ is the DC current, $v_{gs} = V_{gs} - V_{GS}$ and $v_{ds} = V_{ds} - V_{DS}$, and $Gm2, Gmd, \dots, Gd3$ are the second and third order coefficients that can be identified with the corresponding partial derivatives. In a similar fashion we have [5]:

$$\begin{aligned} Q_g(V_{gs}, V_{ds}) &= Q_g(V_{GS}, V_{DS}) + \frac{\partial Q_g}{\partial V_{gs}} v_{gs} + \frac{\partial Q_g}{\partial V_{ds}} v_{ds} + \frac{\partial^2 Q_g}{\partial V_{gs}^2} v_{gs}^2 + \frac{\partial^2 Q_g}{\partial V_{gs} \partial V_{ds}} v_{gs} \cdot v_{ds} + \frac{\partial^2 Q_g}{\partial V_{ds}^2} v_{ds}^2 + \dots = \\ &= Q_g(V_{GS}, V_{DS}) + Cgs \cdot v_{gs} + Cgd \cdot v_{gd} + Cgs2 \cdot v_{gs}^2 + Cgsd \cdot v_{gs} \cdot v_{gd} + Cgd2 \cdot v_{gd}^2 + \\ &\quad + Cgs3 \cdot v_{gs}^3 + Cgs2gd \cdot v_{gs}^2 \cdot v_{gd} + Cgsd2 \cdot v_{gs} \cdot v_{gd}^2 + Cgd3 \cdot v_{gd}^3 + \dots \end{aligned} \quad (2)$$

In this paper we concentrate on the I/V characteristics and compare the first, second and third order derivatives for three different models: *COBRA*[1], *Statz-Raytheon*[7] and a *modified Materka* model. The analysis shows how the *COBRA* I/V model function and its derivatives are continuous around the entire bias plane, as opposed to the other models which are discontinuous in critical bias regions such as knee, pinch-off or $V_{ds}=0V$. The consequences of these differences are clearly seen in the IMD test results presented in the last section, where third and fifth IM products are seen to be very poorly described by the *Statz-Raytheon* and the *modified Materka* models. All these tests have been performed at four different bias conditions which have been specially chosen in the vicinity of those critical areas mentioned above.

IM DISTORTION PREDICTION CAPABILITIES OF FET MODELS

Most of the existing FET models, although they can predict relatively well the I/V characteristics, they fail to a large extent to reproduce the corresponding high-order derivatives. Moreover, for many of these models, where the I/V characteristics are described by different functions within different bias ranges, those derivatives are not even continuous in certain regions of the bias plane. Those problems are overcome by the novel I_{ds} function used by the *COBRA* model. This model function (3) describes very well the FET's behaviour all around the bias spectrum: linear, knee and the saturation regions, reverse bias region; it can also describe soft breakdown and mild second knee behaviour; it converges smoothly towards zero, when V_{gs} drops below pinch-off; has the ability to follow the negative slope seen in real FETs in the saturation region at high values of the gate voltage, due to electron traps and self heating effects. The model function is continuous over the entire bias plane and its derivatives are also continuous. This function is:

$$I_{ds}(V_{GS}, V_{DS}) = \beta \cdot V_{eff}^{\frac{\lambda}{1 + \mu \cdot V_{DS}^2 + \xi \cdot V_{eff}}} \cdot \tanh[\alpha \cdot V_{DS} \cdot (1 + \zeta \cdot V_{eff})]$$

$$V_{eff} = \frac{1}{2} \left(V_{gst} + \sqrt{V_{gst}^2 + \delta^2} \right)$$

$$V_{gst} = V_{GS} - (1 + \beta_r^2) V_{T0} + \gamma \cdot V_{DS}$$
(3)

where V_{T0} is the pinch-off voltage and $\alpha, \beta, \beta_r, \gamma, \delta, \lambda, \mu, \xi, \zeta$, are model parameters. β_r is a dimensionless parameter, numerically equal with β (when I_{ds} is expressed in Amperes).

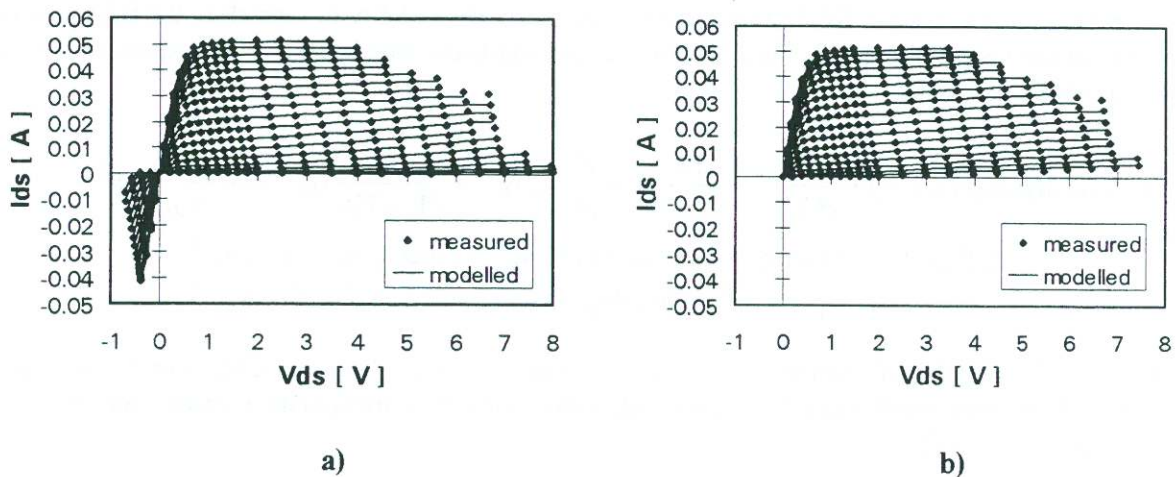


Figure 1. Measured vs. modelled I/V characteristics for a $0.2 \times 120 \mu\text{m}$ PHEMT: (a) *COBRA* ($V_{gs} = -1.4V$ to $+0.6V$; $V_{po} = -1.0V$); (b) *Modified Materka* ($V_{gs} = -1.0V$ to $+0.6V$).

In Figure 1.a we compare measured and modelled (*COBRA*) DC characteristics for a $0.2 \times 120 \mu\text{m}$ PHEMT device (*Philips*). In Figure 1.b, the same data are compared with a *modified Materka* model. An important

shortcoming of the *Materka* model (and indeed of the *Statz-Raytheon*, and most of the other models available) is the restricted bias range over which the I/V model function and its derivatives are defined and continuous. In practice it is very hard to see significant differences between the two DC models just by looking at the two data-fits in Figure 1, within the normal operating regions. However, things are looking different when the derivatives of the main model functions are analysed and compared. For the three extracted models we calculated the first, second and third derivatives with respect to V_{gs} . Results are presented in Figure 2 (*COBRA*) and Figure 3 (*Materka*). By simple comparison with the results shown in [3][4], it is clear that the *COBRA* model predictions are very similar with what it is expected. All derivatives are seen to be continuous over the entire bias plane.

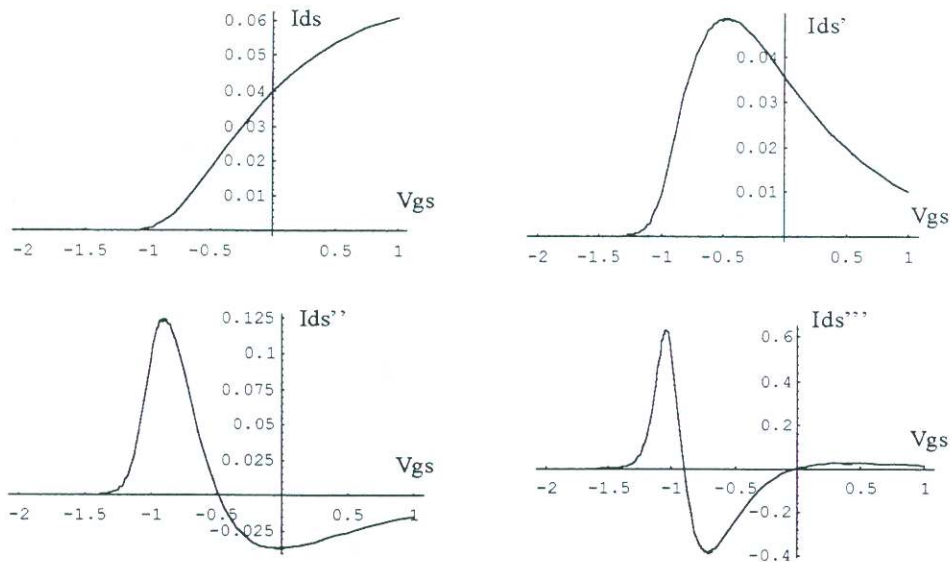


Figure 2. The calculated derivatives of the drain current function for the *COBRA* model ($0.2 \times 120 \mu\text{m}$ PHEMT process with $V_{po} = -1.0V$; $V_{ds} = 3.0V$)

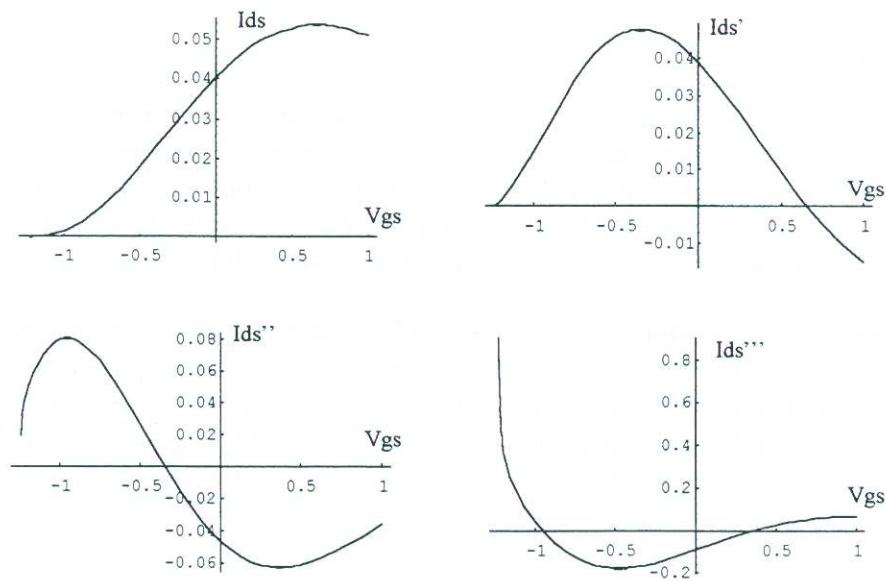


Figure 3. The calculated derivatives of the drain current function for the *modified Materka* model ($0.2 \times 120 \mu\text{m}$ PHEMT process with $V_{po} = -1.0V$; $V_{ds} = 3.0V$)

A similar study has been performed in relation to the Q/V characteristics. In this respect *COBRA* and *Statz-Raytheon* models show much better performance in comparison to *Materka model* which uses the simple diode capacitance model. A comparison between the calculated first, second and third order derivatives of the gate charge functions used in *COBRA* and *Materka* models is shown in Figure 4.a,b. A simple comparison with the measured results for similar devices published in [5], confirms the superiority of the *COBRA* charge and capacitance models. Another strength of the *COBRA* model in comparison to other models, that also contributes to its enhanced IMD prediction capabilities, is given by the consistent account of DC/AC dispersion effects as it has been described in detail in [1][6].

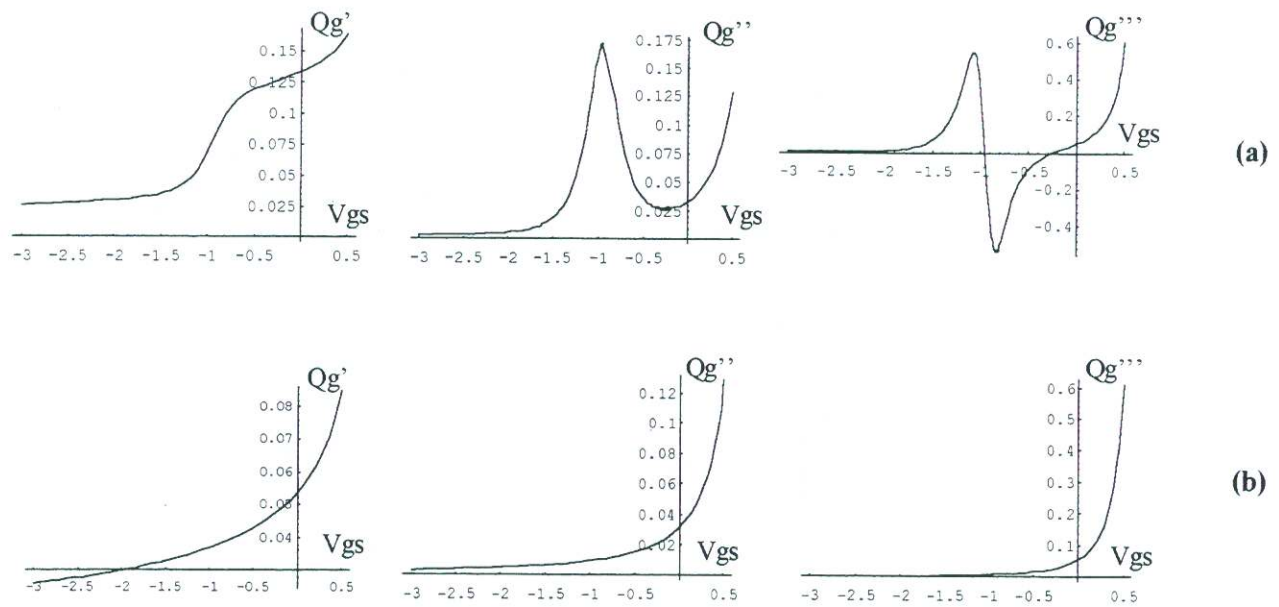


Figure 4. The calculated derivatives of the gate charge function for the *COBRA* (a) and the *Materka* (b) models ($0.2 \times 120 \mu\text{m}$ PHEMT process with $V_{po} = -1.0V$; $V_{ds} = 3.0V$)

TEST RESULTS

A comprehensive set of two-tone large-signal tests have been carried out in order to validate the overall IMD prediction capabilities of the three models. The tests have been performed on devices from a $0.2 \mu\text{m}$ PHEMT process designed for *mm*-wave applications (30-50GHz band). We carried out the tests at four different bias conditions, some of them specially selected in the neighbourhood of those critical bias regions mentioned previously. The frequencies of the two tones used have been around 9.0GHz.

The simulations have been performed within the HP-MDS framework. Results for the case of a $0.2 \times 120 \mu\text{m}$ PHEMT are presented in Figure 5.a,b,c, for the *COBRA*, *Statz-Raytheon* and *modified Materka* models, respectively. Similar tests have been repeated for a $300 \mu\text{m}$ device in order to test the scalability of the models. All results show a very good overall agreement between the experimental and simulated IMD characteristics for the case of *COBRA* model and much poorer results for the high order IM products in the case of the other two models.

ACKNOWLEDGEMENTS

This work has been partly supported by the *ESPRIT-EDGE* project. The authors would like to thank Dr. Remy Leblanc of Philips Microwave Limeil, France, for providing the PHEMT devices used in our tests.

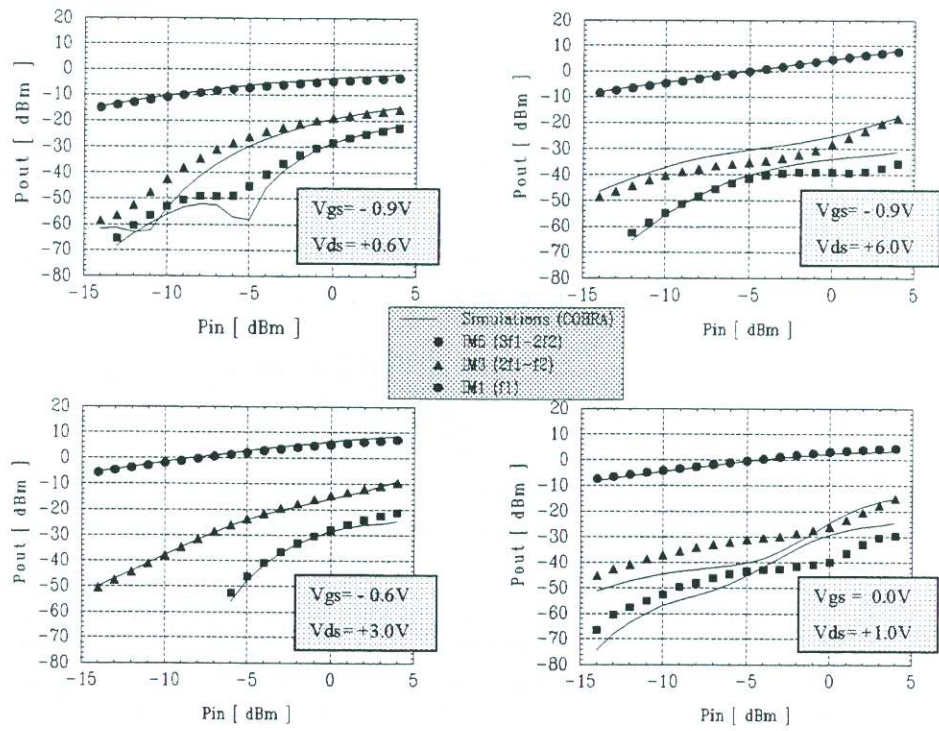


Figure 5.a. Experimental vs. calculated IMD characteristics using the *COBRA* model (0.2x120 μ m PHEMT process with $f_1=8.975$ GHz and $f_2=9.015$ GHz ($V_{po} = -1.0$ V))

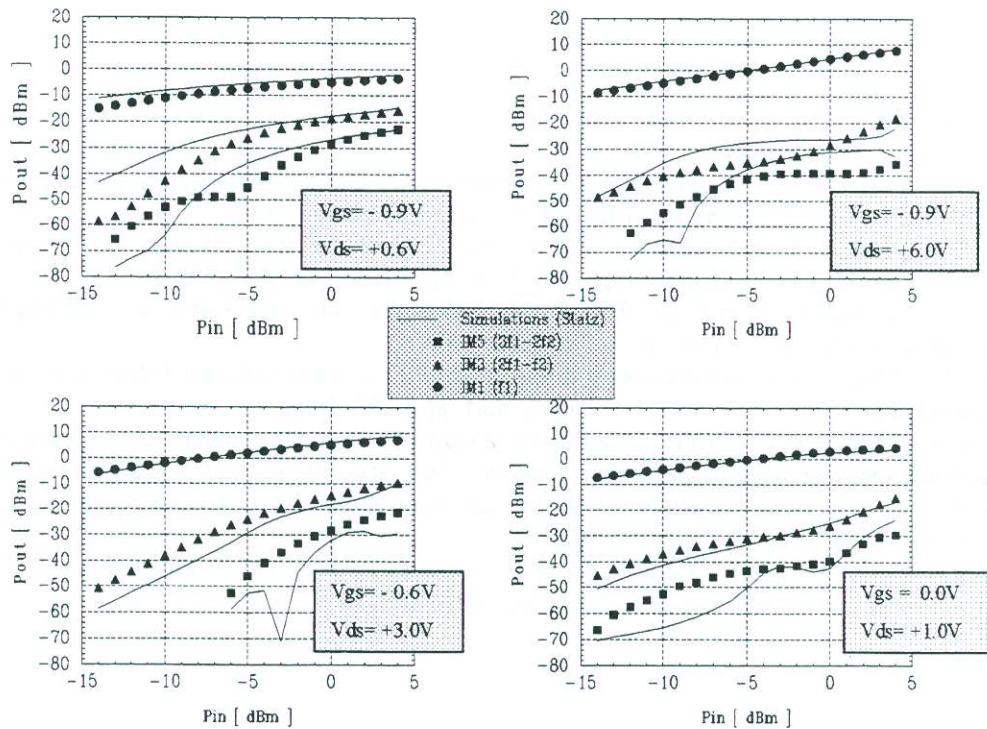


Figure 5.b. Experimental vs. calculated IMD characteristics using the *Statz-Raytheon* model (0.2x120 μ m PHEMT process with $f_1=8.975$ GHz and $f_2=9.015$ GHz ($V_{po} = -1.0$ V))

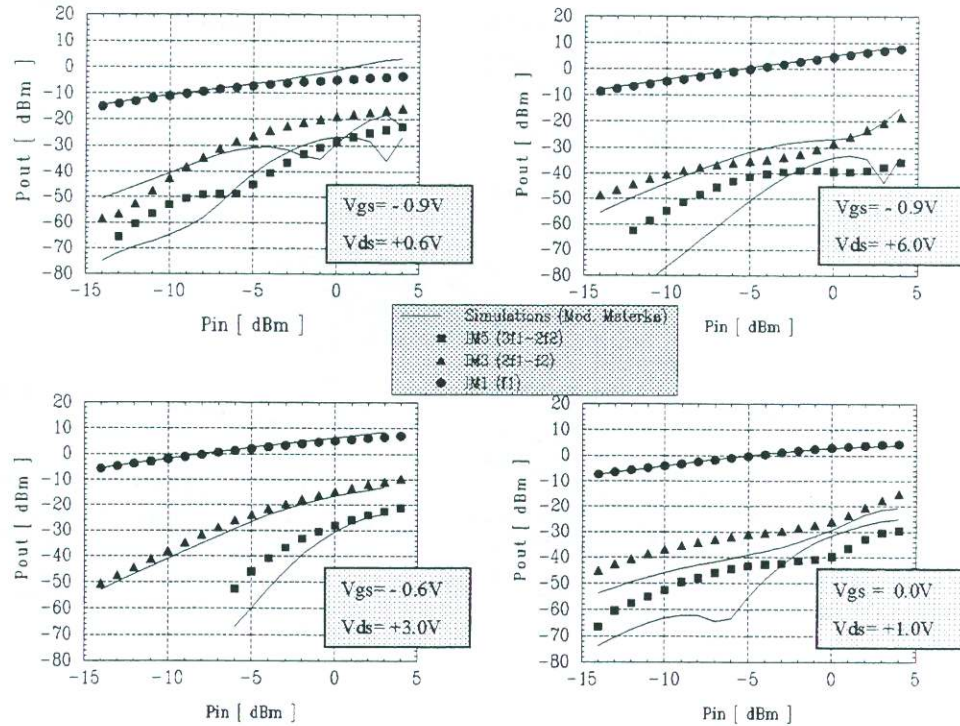


Figure 5.c. Experimental vs. calculated IMD characteristics using the *Modified Materka* model (0.2x120 μ m PHEMT process with $f_1=8.975\text{GHz}$ and $f_2=9.015\text{GHz}$; $V_{po} = -1.0\text{V}$)

REFERENCES

- [1] Cojocaru V.I., Brazil T.J., "A scalable general-purpose model for microwave FET's including the DC/AC dispersion effects", *IEEE Trans. on MTT*, Vol. 45, No. 12, December 1997.
- [2] Maas S.A., Crosmun A., "Modelling the gate I/V characteristic of a GaAs MESFET for Volterra-series analysis", *IEEE Trans. on MTT*, Vol. 37, No. 7, pp. 1134-1136, July 1989.
- [3] Maas S.A., Neilson D., "Modelling MESFET's for intermodulation analysis of mixers and amplifiers", *IEEE Trans. on MTT*, Vol. 38, pp. 1964-1971, December 1990.
- [4] Pedro J.C., Perez J., "Accurate simulation of GaAs MESFET's intermodulation distortion using new drain-source current model", *IEEE Trans. on MTT*, Vol. 42, No. 1, pp.25-33, January 1994.
- [5] Garcia J.A., Mediavilla A., Tazon A., Garcia J.L., Pedro J.C., "Accurate characterisation procedure of FET's reactive nonlinearities for intermodulation analysis", *Proc. of GAAS'97 Conf.*, pp. 87-90, Bologna, Sept. 1997.
- [6] Cojocaru V.I., Brazil T.J., "Scalability of DC/AC non-linear dispersion models for microwave FET's", *IEEE MTT-S Digest*, pp. 387-390, Denver, 1997.
- [7] Stutz H., Newman P., Smith I., Pucel R., Haus H., "GaAs FET device and circuit simulation in SPICE", *IEEE Trans. On Electron Devices*, Vol. ED-34, pp. 160-169, 1987.